

# Accelerating Conditional Prompt Learning via Masked Image Modeling for Vision-Language Models

Phuoc-Nguyen Bui\*  
 Convergence Research Institute,  
 Sungkyunkwan University  
 Suwon, South Korea

Khanh-Binh Nguyen\*  
 School of Information Technology,  
 Deakin University  
 Geelong, Australia

Hyunseung Choo†  
 Department of Electrical and  
 Computer Engineering,  
 Sungkyunkwan University  
 Suwon, South Korea

## Abstract

Vision-language models (VLMs) like CLIP excel in zero-shot learning but often require resource-intensive training to adapt to new tasks. Prompt learning techniques, such as CoOp and CoCoOp, offer efficient adaptation but tend to overfit to known classes, limiting generalization to unseen categories. We introduce ProMIM, a plug-and-play framework that enhances conditional prompt learning by integrating masked image modeling (MIM) into existing VLM pipelines. ProMIM leverages a simple yet effective masking strategy to generate robust, instance-conditioned prompts, seamlessly augmenting methods like CoOp and CoCoOp without altering their core architectures. By masking only visible image patches and using these representations to guide prompt generation, ProMIM improves feature robustness and mitigates overfitting, all while introducing negligible additional computational cost. Extensive experiments across zero-shot and few-shot classification tasks demonstrate that ProMIM consistently boosts generalization performance when plugged into existing approaches, providing a practical, lightweight solution for real-world vision-language applications.

## CCS Concepts

- Computing methodologies → Computer vision; Image representations.

## Keywords

Vision-language models, Prompt learning, Masked image modeling

### ACM Reference Format:

Phuoc-Nguyen Bui, Khanh-Binh Nguyen, and Hyunseung Choo. 2025. Accelerating Conditional Prompt Learning via Masked Image Modeling for Vision-Language Models. In *Proceedings of the 2nd International Workshop on Large Vision - Language Model Learning and Applications (LAVA '25)*, October 27–31, 2025, Dublin, Ireland. ACM, New York, NY, USA, 10 pages. <https://doi.org/10.1145/XXXXXX.XXXXXX>

\*Both authors contributed equally to this research.

†Corresponding author

Permission to make digital or hard copies of all or part of this work for personal or classroom use is granted without fee provided that copies are not made or distributed for profit or commercial advantage and that copies bear this notice and the full citation on the first page. Copyrights for components of this work owned by others than the author(s) must be honored. Abstracting with credit is permitted. To copy otherwise, or republish, to post on servers or to redistribute to lists, requires prior specific permission and/or a fee. Request permissions from [permissions@acm.org](mailto:permissions@acm.org).

LAVA '25, Dublin, Ireland.

© 2018 Copyright held by the owner/author(s). Publication rights licensed to ACM.

ACM ISBN 979-8-4007-1840-3/2025/10

<https://doi.org/10.1145/XXXXXX.XXXXXX>

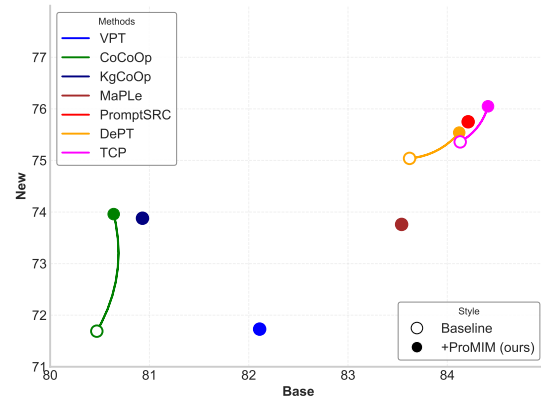
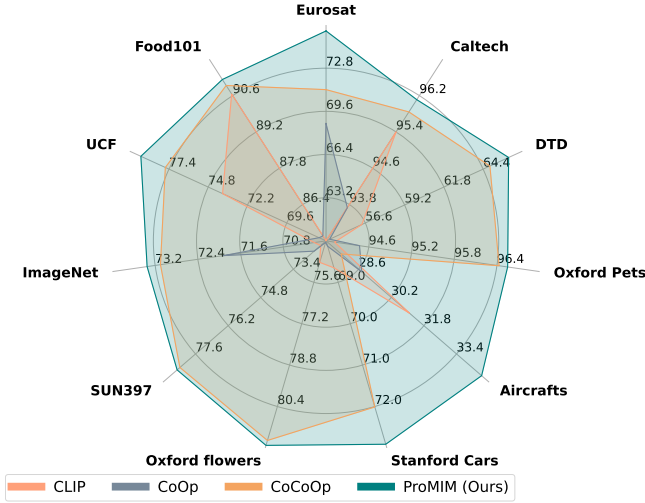


Figure 1: Classification accuracies of six prompt tuning methods w/ or w/o our ProMIM on Base (or seen) and New (or unseen) tasks, averaged over 11 datasets in Table 1.

## 1 Introduction

Vision-language models (VLMs), such as Contrastive Language–Image Pretraining [30] (CLIP), A Large-scale ImaGe and Noisy-text embedding [16] (ALIGN), and Flamingo [1], represent a significant leap in aligning visual and textual representations within a shared embedding space. These models enable zero-shot transfer learning by associating images with descriptive language labels, which provides valuable flexibility for downstream applications. However, training such models often requires large amounts of data and computing resources, which are available primarily to large institutions. For example, CLIP leverages an extensive dataset of image-text pairs, which makes it difficult for smaller research teams to replicate its scale and effectiveness. Furthermore, while large datasets enable high performance, they can also introduce biases or irrelevant information, limiting the generalizability of these models to niche or domain-specific applications.

Prompt learning has emerged as an efficient adaptation strategy for VLMs, inspired by prompt-tuning techniques in natural language processing (NLP) [4, 6, 23, 29, 36]. Through prompt learning, these models can adapt more flexibly to new tasks by embedding additional context-specific information directly into the prompt rather than modifying the entire network. However, prompt-based methods face challenges, especially in maintaining performance on unseen classes. For instance, Context Optimization (CoOp) [45] is prone to overfitting; while it performs well on seen classes, its accuracy drops significantly on unseen classes, often under-performing



**Figure 2: Performance comparison on base-to-novel generalization.**

compared to CLIP’s zero-shot capabilities. This is because CoOp tends to specialize prompts for known classes, which limits model’s generalization capability.

To address this, Zhou et al. [44] introduced Conditional Context Optimization (CoCoOp) method with instance-conditioned prompts, aiming to adapt prompts based on the specific features of each instance, enhancing CoOp’s flexibility. Although CoCoOp shows improved generalization on unseen classes, it still suffers from overfitting due to data leakage issues, where prompts trained on seen instances can inadvertently capture information that affects performance on unseen classes [25]. Recently, KgCoOp (Knowledge-guided Context Optimization) [41] was developed to tackle this issue by aligning learnable prompts more closely with hand-crafted prompts, thereby reducing context discrepancies, enhancing prompt stability across diverse tasks and reducing the overfitting problem. However, KgCoOp’s improvements are primarily confined to text features, without fully leveraging the vision encoder’s potential. This lack of integration with visual features limits its capacity to harness the vision-language model’s full representational power.

To address these limitations, we propose Masked Image Modeling-guided Conditional Prompt Learning (ProMIM), a plug-and-play enhancement for prompt learning in VLMs that integrates masked image modeling (MIM) to boost generalization without disrupting existing frameworks as shown in Figure 1. Designed to seamlessly augment methods like CoOp and CoCoOp, ProMIM acts as a modular add-on that enhances their performance while preserving compatibility with pretrained models. By randomly masking image patches and using these representations to guide prompt generation, ProMIM encourages the model to learn robust, domain-invariant features, reducing overfitting to specific visual details. This lightweight approach requires no architectural overhaul—ProMIM simply enhances the input processing stage, making it an easy-to-adopt solution for adapting VLMs. Unlike KgCoOp’s text-centric design, ProMIM leverages masked visual information, unlocking the vision encoder’s full representational power while integrating effortlessly

with existing pipelines. As a result, ProMIM improves adaptability to unseen data and maintains strong performance on seen classes, offering a practical tool for real-world vision-language tasks. The contributions are as follows:

- We present ProMIM, a plug-and-play framework that enhances conditional prompt learning by incorporating masked image modeling, providing a drop-in solution to improve generalization in VLMs.
- Through comprehensive experiments on different configurations, we show that ProMIM consistently elevates the performance of existing CoOp-based methods, achieving superior adaptability to unseen classes.
- We validate the robustness and flexibility of ProMIM across a wide range of datasets, highlighting its potential as a versatile, easy-to-adopt tool for vision-language applications requiring strong generalization.

## 2 Related Work

### 2.1 Visual-Language Models

Recent research highlights that pairing images with associated text, rather than analyzing images alone, can lead to highly effective vision-language models (VLMs). A key example of this approach is CLIP [30], which uses contrastive loss to train both a vision encoder and a text encoder on a dataset of 400 million image-text pairs, demonstrating impressive generalization to unseen classes. Vision-language models like CLIP harness the relationship between images and text, opening up new possibilities for learning generalized visual representations. VLMs have continued to evolve, improving through the use of more advanced text and visual encoders, such as Transformers [9]; contrastive learning techniques [5]; and increasingly large datasets [16]. Since training VLMs typically requires extensive annotated datasets, unsupervised and weakly supervised methods [38] have been explored as alternatives to annotate-free training. Specifically, Masked Language Modeling (MLM) [19, 24] enhances robustness in text and visual embeddings by randomly masking words in text, while Masked Auto-Encoders (MAE) employ self-supervised learning by masking random image patches, facilitating the development of adaptable, domain-agnostic representations that enhance the model’s generalization capacity across diverse tasks and domains.

### 2.2 Prompt Tuning

To customize pretrained VLMs for downstream tasks, prompt tuning [29] integrates task-specific textual tokens to extract relevant knowledge for each task [36]. For instance, CLIP [30] uses a manually crafted template, such as “a photo of a [CLS],” to create textual embeddings for zero-shot inference. However, such hand-crafted prompts can lack expressiveness, as they may not fully capture task-specific nuances. To address this, Context Optimization (CoOp) [45] replaces these static prompts with learnable, soft prompts based on labeled few-shot samples, enhancing adaptability to specific tasks. A limitation of CoOp, however, is that its learnable prompts remain fixed across all images within a task, thus overlooking individual image characteristics. Conditional Context Optimization (CoCoOp) [44] advances this by generating an image-conditioned prompt for each instance, which it combines with a textual-conditioned

context to create task-specific prompts. This approach employs a lightweight neural network to generate an adaptive, learnable text prompt for each image.

Beyond text-only prompt tuning, approaches such as Multimodal Prompt Learning (MaPLe) [17] and PromptSRC [18] incorporate both visual and textual prompt tuning, optimizing jointly across the vision and text encoders. Furthermore, Multi-task Vision-Language Prompt Tuning (MViPT) [33] integrates cross-task knowledge to enhance prompt learning for VLMs, while DenseCLIP [31] employs context-aware prompt adjustments tailored for dense prediction tasks. Another approach, CLIP-Adapter [11], enhances adaptation by introducing adapters that fine-tune both visual and textual embeddings, thus enabling VLMs to better accommodate diverse downstream applications. Recently, CasPL [39] introduces a plug-and-play, two-phase framework—boosting and adapting prompts—to improve generalization with minimal overhead. Unlike CasPL’s two-phase approach, our ProMIM offers a one-phase, plug-and-play method with masked image modeling, building on CoCoOp to enhance robustness and generalization efficiently.

### 3 Methodology

#### 3.1 Prompt learning for CLIP

Prompt learning removes the dependency on manually crafted prompts, such as ‘a photo of a [...]’ to better align with downstream task requirements. The pioneering work, CoOp [45], defines a prompt as a sequence of  $M$  continuously differentiable tokens, denoted by  $[v_1][v_2] \dots [v_M]$ . In the case of the CLIP-ViT architecture, each token  $[v_i]$  is represented as a 512-dimensional vector. Consequently, the prompt for the  $i$ -th class can be formulated as  $t_i(x) = v_1(x), v_2(x), \dots, v_M(x), c_i$ , where  $c_i$  is the class label. Let  $x$  represent the feature embeddings from the image encoder, and  $g(\cdot)$  denote the features from the text encoder. The class probabilities are then computed as follows:

$$p(\hat{y} | x) = \frac{\exp \left( \text{sim} \left( x, g(t_y) \right) / \tau \right)}{\sum_{i=1}^C \exp \left( \text{sim} \left( x, g(t_i) \right) / \tau \right)} \quad (1)$$

Here,  $\text{sim}(\cdot, \cdot)$  denotes a similarity function within the feature space, where cosine similarity is frequently adopted, and  $\tau$  represents the temperature parameter controlling the concentration of the distribution. Conditional Context Optimization (CoCoOp) [44] leverages image-conditioned prompts to improve generalization across unseen categories by dynamically adapting to input image features. Specifically, these image-conditioned prompts,  $t_i(x) = v_1(x), v_2(x), \dots, v_M(x), c_i$ , are computed by combining meta-tokens  $\pi$  generated by a ‘meta-network’  $h_\theta$  with the token sequence  $[v_i]$ . The class probabilities are defined as:

$$p(\hat{y} | x) = \frac{\exp \left( \text{sim} \left( x, g(t_y(x)) \right) / \tau \right)}{\sum_{i=1}^C \exp \left( \text{sim} \left( x, g(t_i(x)) \right) / \tau \right)} \quad (2)$$

Both CoOp and CoCoOp update token representations; however, CoCoOp further optimizes the meta-network parameters  $h_\theta$  using

cross-entropy loss derived from the downstream task objectives described as follows:

$$\mathcal{L}_{\text{ce}}(y, \hat{y}) = - \sum_{i=1}^C y_i \log (\hat{y}_i) \quad (3)$$

Yao et al. [41] presents Knowledge-guided Context Optimization (KgCoOp) as a method to improve the generalizability of learnable prompts for classes not encountered during training. This is achieved by reducing the difference between textual embeddings produced by the learned prompts and those created with handcrafted prompts. One of the primary limitations of current fine-tuning techniques is the substantial reduction in zero-shot generalization when newly introduced learnable parameters are specifically adapted for a downstream task, often resulting in overfitting to the downstream dataset. In the subsequent section, we present ProMIM, a novel framework designed to mitigate this issue by enhancing both downstream task performance and zero-shot prediction capabilities.

#### 3.2 ProMIM

**Motivation.** While CoCoOp demonstrates impressive performance, a notable limitation is its tendency to be overly confident with unfamiliar classes. We conjecture that this challenge arises from utilizing image features created by the visual path, which are then transferred to the textual path to produce prompts. This technique increases the potential for data leakage because features from the visual side may leak to the textual side and lead the model to overfit to the training data, thereby diminishing its adaptability and ultimately compromising its generalizability.

A straightforward remedy is employing distinct encoders for various augmented input images to enhance diversity. However, as demonstrated in [22], even with image flipping, CLIP maintains identical cosine similarity. Consequently, utilizing different augmented input images with separate encoders is rendered ineffective.

**Masked Image Modeling as a regularization.** ProMIM tackles the drawback of poor generalization due to overfitting on the downstream tasks by implementing a masked image modeling strategy to conventional prompt learning. To prevent the data leakage issue from happening, we randomly mask the input image before inputting it to the image encoder. ProMIM prevents the model from remembering the global information in training data, and the model is encouraged to learn more generalized features that are applicable to a wider range of images.

In addition, using masked image features to generate the context tokens, rather than relying on full image features, can enhance robustness. The masked features force the model to learn from incomplete information, making it more resilient to variations and occlusions in the image [20, 34]. By focusing on these masked features, the model is encouraged to capture the core, essential characteristics of objects and scenes, thereby improving its generalization ability to unseen classes. However, utilizing the same image encoder for both the full image and the masked image to generate context tokens is inefficient, as it requires processing the data twice—once for the full image and again for the masked image—before performing backward propagation. This redundant processing increases computational overhead and limits efficiency.

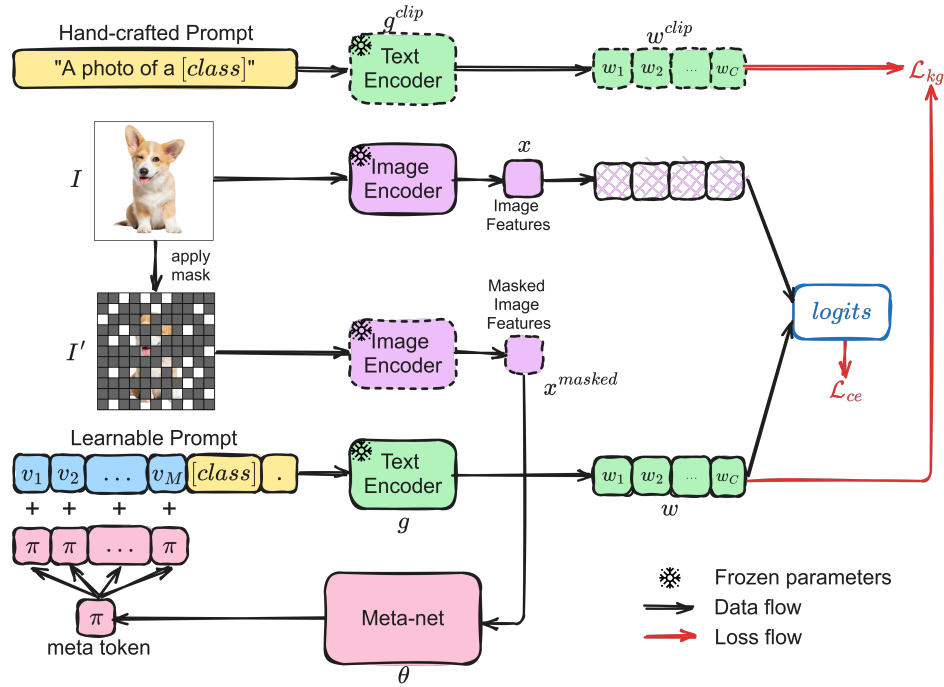


**Figure 3: The framework of the proposed ProMIM. The masked input image embedding is used to generate the learnable meta token that integrates with the learnable context tokens. Thus, ProMIM mitigates the overfitting caused by data leakage.**

To address this issue, we utilize the powerful generalized CLIP as the individual encoder, as depicted in Figure 3. We use the pre-trained CLIP image encoder for image encoding. Initially, the image  $I$  is segmented into a grid consisting of non-overlapping patches. A substantial number of these patches (e.g., 50% or 75%) are randomly masked to obtain the masked image  $I'$ , where the image encoder processes only the visible patches, following the approach in [12]. By applying a masking ratio of 50% (or 75%), the computational overhead for masked image encoding is reduced to half (or quarter), and this adjustment also allows the utilization of a batch size while maintaining a similar memory requirement for image encoding.

Let  $h_\theta(\cdot)$  represents the meta-net parameterized by  $\theta$ , where each context token is now computed as  $v_m(x^{\text{masked}}) = v_m + \pi$ , with  $\pi = h_\theta(x^{\text{masked}})$  and  $m \in \{1, 2, \dots, M\}$ . Consequently, the prompt for the  $i$ -th class becomes conditioned on the masked input, formulated as  $t_i(x^{\text{masked}}) = \{v_1(x^{\text{masked}}), v_2(x^{\text{masked}}), \dots, v_M(x^{\text{masked}}), c_i\}$ . During training, both the context vectors  $v_m$  and the parameters  $\theta$  of the meta-network are jointly updated. The prediction probability from Equation 2 is then modified as follows:

$$p(\hat{y} | x) = \frac{\exp \left( \text{sim} \left( x, g \left( t_y(x^{\text{masked}}) \right) \right) / \tau \right)}{\sum_{i=1}^C \exp \left( \text{sim} \left( x, g \left( t_i(x^{\text{masked}}) \right) \right) / \tau \right)} \quad (4)$$

To strengthen regularization under the consistency constraint, we utilize the standard CLIP text encoder and apply regularization of KgCoOp. We define the text embeddings produced by CLIP and

ProMIM as  $w_i^{\text{clip}} = g^{\text{clip}}(t_i^{\text{clip}})$  and  $w_i^{\text{ProMIM}} = g(t_i)$ , respectively.  $t_i^{\text{clip}} = e(\text{"a photo of a [CLS]"}^{\text{clip}})$  represents the vectorized textual tokens in CLIP of the  $i$ -th class template "a photo of a [CLS]", while  $g^{\text{clip}}$  and  $g$  denote the text encoders for the hand-crafted prompt and the soft prompt, respectively. In line with KgCoOp, we aim to decrease the distance between  $w_i^{\text{ProMIM}}$  and  $w_i^{\text{clip}}$  to enhance the generalizability of the unseen classes.

$$\mathcal{L}_{kg} = \frac{1}{N_c} \sum_{i=1}^{N_c} \|w_i^{\text{ProMIM}} - w_i^{\text{clip}}\|_2^2 \quad (5)$$

where  $\|\cdot\|$  denotes the Euclidean distance, and  $N_c$  represents the number of seen classes. The final objective is:

$$\mathcal{L} = \mathcal{L}_{ce} + \lambda \mathcal{L}_{kg} \quad (6)$$

where  $\lambda$  serves as a balancing factor for the influence of  $\mathcal{L}_{kg}$  in the overall objective function.

## 4 Experiments

Our approach is comprehensively evaluated across three configurations: 1) generalization from base classes to novel classes within the same dataset, 2) cross-dataset transferability, and 3) domain generalization. All models utilized in our experiments are implemented using the open-source CLIP framework [30].

**Datasets.** For the initial two configurations, namely base-to-new generalization and cross-dataset transferability, we utilized the 11 image recognition datasets detailed in [45], which span a broad spectrum of recognition tasks. This benchmark includes ImageNet [8]

**Table 1: Quantitative comparison with existing methods under the base-to-new generalization setting with ViT-B/16 as the backbone on 11 datasets. The context length  $M$  is set to 4 for prompt-based approaches, with 16-shot samples drawn from the base classes. H: Harmonic mean.**

(a) Average over 11 datasets.				(b) ImageNet.				(c) Caltech.				(d) Pets.			
ViT-B/16	Base	New	H	ViT-B/16	Base	New	H	ViT-B/16	Base	New	H	ViT-B/16	Base	New	H
CLIP	69.34	74.22	71.70	CLIP	72.43	68.14	70.22	CLIP	96.84	94.00	95.40	CLIP	91.17	97.26	94.12
CoOp	82.69	63.22	71.66	CoOp	76.47	67.88	71.92	CoOp	98.00	89.81	93.73	CoOp	93.67	95.29	94.47
KgCoOp	80.73	73.60	77.00	KgCoOp	75.83	69.96	72.78	KgCoOp	97.72	94.39	96.03	KgCoOp	94.65	97.76	96.18
ProGrad	82.48	70.75	76.16	ProGrad	77.02	66.66	71.46	ProGrad	98.02	93.89	95.91	ProGrad	95.07	97.63	96.33
MaPLe	82.28	75.14	78.55	MaPLe	76.66	70.74	73.47	MaPLe	97.74	94.36	96.02	MaPLe	95.43	97.76	96.58
PromptSRC	84.26	76.10	79.97	PromptSRC	77.60	70.73	74.01	PromptSRC	98.10	94.03	96.02	PromptSRC	95.33	97.30	96.30
CoCoOp	80.47	71.69	75.83	CoCoOp	75.98	70.43	73.10	CoCoOp	97.96	93.81	95.84	CoCoOp	95.20	97.69	96.43
+ProMIM	<b>80.64</b>	<b>73.96</b>	<b>77.16</b>	+ProMIM	<b>76.12</b>	<b>70.77</b>	<b>73.35</b>	+ProMIM	<b>98.03</b>	<b>94.27</b>	<b>96.11</b>	+ProMIM	<b>95.37</b>	<b>97.76</b>	<b>96.55</b>
DePT	83.62	75.04	79.10	DePT	77.03	70.13	73.42	DePT	98.30	94.60	96.41	DePT	94.33	97.23	96.46
+ProMIM	<b>84.12</b>	<b>75.54</b>	<b>79.60</b>	+ProMIM	<b>77.23</b>	<b>70.23</b>	<b>73.56</b>	+ProMIM	<b>98.32</b>	<b>94.67</b>	<b>96.46</b>	+ProMIM	<b>95.22</b>	<b>97.73</b>	<b>95.78</b>
TCP	84.13	75.36	79.51	TCP	77.27	69.87	73.38	TCP	98.23	94.67	96.42	TCP	94.67	97.20	95.92
+ProMIM	<b>84.41</b>	<b>76.05</b>	<b>80.01</b>	+ProMIM	<b>77.43</b>	<b>70.63</b>	<b>73.88</b>	+ProMIM	<b>98.34</b>	<b>94.89</b>	<b>96.58</b>	+ProMIM	<b>94.87</b>	<b>97.53</b>	<b>96.18</b>
(e) Cars.				(f) Flowers.				(g) Food.				(h) FGVC.			
ViT-B/16	Base	New	H	ViT-B/16	Base	New	H	ViT-B/16	Base	New	H	ViT-B/16	Base	New	H
CLIP	63.37	74.89	68.65	CLIP	72.08	77.80	74.83	CLIP	90.10	91.22	90.66	CLIP	27.19	36.29	31.09
CoOp	78.12	60.40	68.13	CoOp	97.60	59.67	74.06	CoOp	88.33	82.26	85.19	CoOp	40.44	22.30	28.75
KgCoOp	71.76	75.04	73.36	KgCoOp	95.00	74.73	83.65	KgCoOp	90.50	91.70	91.09	KgCoOp	36.21	33.55	34.83
ProGrad	77.68	68.63	72.88	ProGrad	95.54	71.87	82.03	ProGrad	90.37	89.59	89.98	ProGrad	40.54	27.57	32.82
MaPLe	72.94	74.00	73.47	MaPLe	95.92	72.46	82.56	MaPLe	90.71	92.05	91.38	MaPLe	37.44	35.61	36.50
PromptSRC	78.27	74.97	76.58	PromptSRC	98.07	76.50	85.95	PromptSRC	90.67	91.53	91.10	PromptSRC	43.73	37.87	40.15
CoCoOp	70.49	73.59	72.01	CoCoOp	94.87	71.75	81.71	CoCoOp	<b>90.70</b>	91.29	90.99	CoCoOp	33.41	23.71	27.74
+ProMIM	<b>71.67</b>	<b>74.20</b>	<b>72.91</b>	+ProMIM	<b>94.93</b>	<b>72.01</b>	<b>81.90</b>	+ProMIM	90.67	<b>91.77</b>	<b>91.22</b>	+ProMIM	<b>35.70</b>	<b>33.63</b>	<b>34.63</b>
DePT	79.13	75.47	77.26	DePT	98.00	76.37	85.84	DePT	90.50	91.60	91.05	DePT	43.20	34.83	38.57
+ProMIM	<b>79.40</b>	<b>75.63</b>	<b>77.47</b>	+ProMIM	<b>98.20</b>	<b>76.73</b>	<b>86.15</b>	+ProMIM	<b>90.77</b>	<b>91.77</b>	<b>91.27</b>	+ProMIM	<b>43.56</b>	<b>34.91</b>	<b>38.76</b>
TCP	80.80	74.13	77.32	TCP	97.73	75.57	85.23	TCP	90.57	91.37	90.97	TCP	41.97	34.43	37.83
+ProMIM	<b>80.93</b>	<b>74.37</b>	<b>77.51</b>	+ProMIM	<b>98.13</b>	<b>75.77</b>	<b>85.51</b>	+ProMIM	<b>90.73</b>	<b>91.50</b>	<b>91.11</b>	+ProMIM	<b>42.12</b>	<b>36.83</b>	<b>39.30</b>
(i) SUN397.				(j) DTD.				(k) EuroSAT.				(l) UCF101.			
ViT-B/16	Base	New	H	ViT-B/16	Base	New	H	ViT-B/16	Base	New	H	ViT-B/16	Base	New	H
CLIP	69.36	75.35	72.23	CLIP	53.24	59.90	56.37	CLIP	56.48	64.05	60.03	CLIP	70.53	77.50	73.85
CoOp	80.60	65.89	72.51	CoOp	79.44	41.18	54.24	CoOp	92.19	54.74	68.69	CoOp	84.69	56.05	67.46
KgCoOp	80.29	76.53	78.36	KgCoOp	77.55	54.99	64.35	KgCoOp	85.64	64.34	73.48	KgCoOp	82.89	76.67	79.65
ProGrad	81.26	74.17	77.55	ProGrad	77.35	52.35	62.45	ProGrad	90.11	60.89	72.67	ProGrad	84.33	74.94	79.35
MaPLe	80.82	78.70	79.75	MaPLe	80.36	59.18	68.16	MaPLe	94.07	73.23	82.35	MaPLe	83.00	78.66	82.35
PromptSRC	82.67	78.47	80.52	PromptSRC	83.37	62.97	71.75	PromptSRC	92.90	73.90	82.32	PromptSRC	87.10	78.80	82.74
CoCoOp	79.74	76.86	78.27	CoCoOp	77.01	56.00	64.85	CoCoOp	<b>87.49</b>	60.04	71.21	CoCoOp	<b>82.33</b>	73.45	77.64
+ProMIM	<b>79.91</b>	<b>76.93</b>	<b>78.39</b>	+ProMIM	<b>77.47</b>	<b>57.63</b>	<b>66.09</b>	+ProMIM	84.97	<b>68.03</b>	<b>75.56</b>	+ProMIM	82.23	<b>76.50</b>	<b>79.26</b>
DePT	82.33	77.80	80.00	DePT	82.20	59.13	68.78	DePT	89.03	71.07	79.04	DePT	85.80	77.23	81.29
+ProMIM	<b>82.43</b>	<b>77.97</b>	<b>80.14</b>	+ProMIM	<b>83.13</b>	<b>61.60</b>	<b>70.76</b>	+ProMIM	<b>91.30</b>	<b>71.87</b>	<b>80.43</b>	+ProMIM	<b>85.80</b>	<b>77.87</b>	<b>81.64</b>
TCP	82.63	78.20	80.35	TCP	82.77	58.07	68.25	TCP	91.63	74.73	82.32	TCP	87.13	80.77	83.83
+ProMIM	<b>82.69</b>	<b>78.35</b>	<b>80.46</b>	+ProMIM	<b>83.63</b>	<b>60.73</b>	<b>66.94</b>	+ProMIM	<b>91.82</b>	<b>74.99</b>	<b>82.56</b>	+ProMIM	<b>87.83</b>	<b>80.97</b>	<b>84.26</b>

**Table 2: Comparison in the cross-dataset transfer setting. The source model is trained on ImageNet [8].**

Method	Source	Target										Avg.
		ImageNet	Caltech	Pets	Cars	Flowers	Food	FGVC	SUN397	DTD	EuroSAT	UCF101
CoOp	71.51	93.70	89.14	64.51	68.71	85.30	18.47	64.15	41.92	46.39	66.55	63.88
CoCoOp	<b>71.02</b>	<b>94.43</b>	90.14	<b>65.32</b>	<b>71.88</b>	86.06	22.94	67.36	45.73	45.37	<b>68.21</b>	65.74
<b>+ProMIM</b>	70.60	93.97	<b>90.33</b>	65.03	71.47	<b>86.67</b>	<b>23.87</b>	<b>67.40</b>	<b>47.60</b>	<b>46.77</b>	67.80	<b>66.09</b>
DePT	<b>72.77</b>	94.10	<b>90.63</b>	<b>66.23</b>	<b>72.17</b>	86.27	22.90	<b>67.30</b>	45.50	44.17	<b>69.53</b>	65.88
<b>+ProMIM</b>	72.53	<b>94.13</b>	90.03	65.40	69.97	<b>86.50</b>	<b>23.70</b>	66.83	<b>46.80</b>	<b>49.85</b>	68.13	<b>66.14</b>
TCP	<b>71.40</b>	93.97	91.25	64.69	<b>71.21</b>	86.69	23.45	<b>67.15</b>	44.35	51.45	68.73	66.29
<b>+ProMIM</b>	71.23	<b>94.03</b>	<b>91.33</b>	<b>65.20</b>	71.11	<b>86.86</b>	<b>23.79</b>	66.64	<b>46.20</b>	<b>51.85</b>	<b>68.93</b>	<b>66.59</b>

and Caltech101 (Caltech) [10] for generic object classification; OxfordPets (Pets) [28], StanfordCars (Cars) [21], Flowers102 (Flowers) [27], Food101 (Food) [3], and FGVC Aircraft (FGVC) [26] for fine-grained classification; SUN397 [40] for scene recognition; UCF101 [35] for action recognition; DTD [7] for texture classification; and EuroSAT [13] for satellite image recognition. In the domain generalization setup, we used ImageNet as the source dataset, with four domain-shifted ImageNet variants serving as target datasets: ImageNet-V2 [32], ImageNet-Sketch [37], ImageNet-A [15], and ImageNet-R [14]. Following the protocol described in [45], we randomly selected a few-shot training subset from each dataset, utilizing the original test set for evaluation. To validate the effectiveness of our approach, we conducted experiments with the maximum shot count considered in [45], specifically 16-shot, and reported results averaged over three independent runs.

**Baselines.** We compare our ProMIM against several state-of-the-art methods, including zero-shot and linear probe CLIP [30], CoOp [45], CoCoOp [44], DePT [43], and TCP [42]. For a fair comparison, the baseline results are directly sourced from their respective original publications.

**Implementation details.** Our implementation builds upon the CoCoOp codebase, utilizing CLIP (ViT-B/16) [30] as the pre-trained vision-language model for evaluation. We fine-tune the model in a few-shot setting with 16 samples per class, employing an SGD optimizer over 10 epochs with a batch size of 1 and a learning rate of 0.02. To ensure consistency, we limit the number of context tokens to 4. We report the average accuracy over three independent runs for each experimental setup. The training and evaluation processes are performed on a single NVIDIA H100 GPU, completing within a day for all 11 datasets. The hyperparameter  $\lambda$  is set to 2.0.

#### 4.1 Generalization From Base to New Classes

The main focus of this study is to solve the problem of overfitting in CoCoOp methods. Following the previous methods [17, 41–46], we split each data set into the *Base* and *New* classes. The models are trained on the *Base* classes and evaluated on the test sets of the *Base* and *New* classes. The detailed results are presented in Table 1.

As demonstrated in Table 1, ProMIM achieves a 73.96% accuracy, significantly outperforming CoOp and CoCoOp on the *New*

benchmarks. This improvement can be attributed to ProMIM's ability to mitigate data leakage by utilizing masked image features to generate context tokens, which in turn enhances generalization to unseen classes. Although ProMIM's performance on the *Base* setting is slightly lower, due to the additional regularization applied to reduce overfitting and improve generalization, it demonstrates substantial gains over previous state-of-the-art methods across challenging datasets, including ImageNet, StanfordCars, Oxford Flowers, FGVC Aircraft, DTD, and EuroSAT, where there remains optimization potential. Notably, applying ProMIM to enhance DePT and TCP results in further performance improvements, with accuracies of 84.12% for *Base* classes and 75.54% for *New* classes with DePT and 84.41% and 76.05% for *Base* and *New* classes with TCP, respectively. This enhanced performance underscores the plug-and-play versatility of the proposed ProMIM method, facilitating seamless integration with existing methods.

**Table 3: Comparison of manual and learning-based prompts in domain generalization.**

Method	Source	Target					Avg.
		ImageNet	-V2	-Sketch	-A	-R	
CLIP	66.73	60.83	46.15	47.77	73.96	57.17	
CoOp	71.51	64.20	47.99	49.71	75.21	59.28	
CoCoOp	<b>71.02</b>	64.07	48.75	50.63	76.18	59.90	
<b>+ProMIM</b>	70.60	<b>64.12</b>	<b>48.84</b>	<b>50.85</b>	<b>76.63</b>	<b>60.11</b>	
DePT	-	-	-	-	-	-	-
<b>+ProMIM</b>	<b>72.53</b>	63.97	45.67	46.30	73.00	57.23	
TCP	71.20	64.60	49.50	<b>51.20</b>	76.73	60.51	
<b>+ProMIM</b>	<b>71.23</b>	<b>64.65</b>	<b>49.51</b>	51.11	<b>77.01</b>	<b>60.57</b>	

#### 4.2 Cross-Dataset Transferability Evaluation

To further assess the generalization capability of the ProMIM framework, we conduct a cross-dataset evaluation by training all models on ImageNet and directly testing on 10 additional downstream datasets. The comparative results between ProMIM and existing methods are presented in Table 2. As shown in Table 2, ProMIM

**Table 4: Comparison of average performance across all 11 datasets in the base-to-new setting with varying  $K$ -shot samples.**

Backbones	Methods	K=4			K=8			K=16		
		Base	New	H	Base	New	H	Base	New	H
ViT-B/16	CoOp	78.43	68.03	72.44	<b>80.73</b>	68.39	73.50	<b>82.63</b>	67.99	74.60
	CoCoOp	76.72	73.34	74.85	78.56	72.00	74.90	80.47	71.69	75.83
	ProGrad	79.18	71.14	74.62	80.62	71.02	75.20	82.48	70.75	76.16
	KgCoOp	<b>79.92</b>	73.11	<b>75.90</b>	78.36	73.89	76.06	80.73	73.60	77.00
<b>ProMIM</b>		77.87	<b>76.10</b>	75.62	78.20	<b>74.50</b>	<b>76.30</b>	80.64	<b>73.96</b>	<b>77.16</b>

achieves higher average performance than previous prompt-based methods, including CoOp [45], CoCoOp [44], and DePT [43], which do not integrate prompts deep within the architecture, as seen in methods like MaPLe [17] or TCP [42]. This demonstrates the effectiveness of ProMIM in learning general knowledge. For instance, despite having only 70.60% accuracy on ImageNet, ProMIM achieves an average accuracy of 66.09% across 10 datasets, higher than CoOp, CoCoOp, DePT, and TCP. Furthermore, when DePT and TCP are used with ProMIM, we achieve an average performance higher than those of the existing methods with accuracy improvements of 0.26% and 0.30% overall, respectively.

### 4.3 Domain Generalization

The domain generalization results are summarized in Table 3. Here, the original ImageNet dataset is used as the source for model fine-tuning, followed by the evaluation of four distinct ImageNet variants, each representing a different distribution. As seen in Table 3, ProMIM exhibits slightly lower performance on ImageNet but effectively aligns with performance levels on the target datasets. Notably, when combined with DePT [43], ProMIM achieves peak performance on ImageNet; however, this pairing results in a substantial drop in generalization, indicating a reduced capacity of DePT to generalize across a broader range of unseen classes. In contrast, ProMIM combined with TCP attains the highest overall performance over 4 target datasets.

## 5 Ablation study

### 5.1 Few-shot Classification

To evaluate the effectiveness of the proposed ProMIM, we benchmark its performance against previous prompt-based methods, including CoOp [45], CoCoOp [44], KgCoOp [41], and ProGrad [46], across various backbone models and different  $K$ -shot sample settings. Specifically, we utilize ViT-B/16, a transformer-based deep learning backbone, as the visual encoder for image feature extraction. Additionally, we conduct experiments under three few-shot configurations: 4-shot, 8-shot, and 16-shot. The averaged results are summarized in Table 4. Generally, ProMIM surpasses all methods for the performance on the *New* classes. In particular, ProMIM achieves best performance on *New* classes despite the number of shots. Especially when the number of shots increases, ProMIM surpasses all other methods.

**Table 5: Comparison of average performance across all 11 datasets in the base-to-new setting, with and without the inclusion of MIM-context and  $\mathcal{L}_{kg}$ .**

Methods	MIM context	$\mathcal{L}_{kg}$	Avg 11 datasets		
			Base	New	H
CoOp	$\times$	$\times$	<b>82.63</b>	67.99	74.60
CoCoOp	$\times$	$\times$	80.47	71.69	75.83
ProGrad	$\times$	$\times$	82.48	70.75	76.16
KgCoOp	$\times$	$\checkmark$	80.73	73.60	77.00
<b>ProMIM</b>	$\checkmark$	$\times$	80.40	72.32	76.15
<b>ProMIM</b>	$\checkmark$	$\checkmark$	80.64	<b>73.96</b>	<b>77.16</b>

### 5.2 Impact of each module

Our work focuses on utilizing the features from masked images as a condition for prompt learning, referred to as the MIM context. This approach aims to address the overfitting issue caused by data leakage in CoCoOp method [44]. As demonstrated in Table 5, the inclusion of the MIM context significantly enhances performance compared to CoOp, CoCoOp, KgCoOp, and ProGrad, particularly in the *New* and *H* metrics. Notably, for the *New* performance, incorporating the MIM context results in an improvement of almost 2% over ProGrad. Furthermore, when we apply  $\mathcal{L}_{kg}$  from KgCoOp, the *New* performance exceeds that of KgCoOp, achieving 73.96% compared to 73.60%. This superior performance further validates the effectiveness of using masked image features as a condition, as it helps to prevent overfitting and enhances overall performance over 11 datasets.

### 5.3 Computational Cost

The computational cost of our ProMIM is shown in Table 6a. As observed, the additional computational cost is low (even *negligible*) compared to the performance improvement established by ProMIM. Especially since no additional modules are introduced, the learnable parameters are unchanged.

### 5.4 Mask ratio and $\lambda$ value

We thus confirm the rationale and effectiveness of ProMIM's design, with the relevant results presented in Table 7 and Table 8. Notably, unlike KgCoOp, ProMIM achieves optimal performance at  $\lambda = 2.0$ , indicating that masked image features provide robust regularization. This suggests the need to minimize  $\lambda$  for ProMIM,

**Table 6: Ablation study on computational cost and masking strategy.**

(a) Computational cost of ProMIM. “ms”: millisecond per image. Experiments are performed on an H100 GPU. (b) We compare different masking strategies.

Method	Learnable Parameters	Training time	Inference time	Memory	H (avg)
CoOp	8K	105min	2.78ms	11264MB	71.66
KgCoOp	2K	106min	2.79ms	11254MB	77.00
MaPLE	3635K	111min	2.75ms	11048MB	78.55
CoCoOp	69K	420min	127.06ms	11310MB	75.83
<b>+ProMIM</b>	<b>69K</b>	<b>+3min</b>	<b>+0.1ms</b>	<b>+2MB</b>	<b>77.16 (+0.35)</b>

case	ratio	H (avg)
random	0.50	76.42
random	0.75	<b>77.16</b>
block	0.50	76.31
block	0.75	75.12

whereas KgCoOp requires a larger  $\lambda$  to effectively regularize the loss. Furthermore, when a significant portion of the input image is conditioned, performance declines, likely due to data leakage; the best results are observed when 95% of the input image is masked.

**Table 7: The quantitative analysis of mask ratio on average of 11 datasets.**

mask ratio (%)	0.25	0.5	<b>0.75</b>	0.95	0.99
H	76.21	76.42	<b>77.16</b>	75.36	74.72

**Table 8: Quantitative analysis of  $\mathcal{L}_{kg}$  for varying  $\lambda$  values, averaged over 11 datasets.**

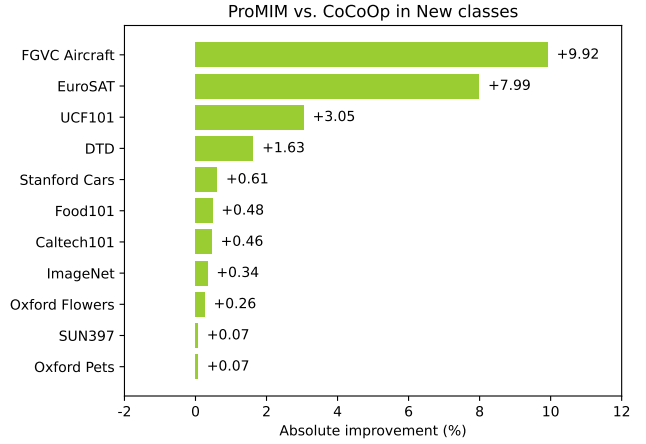
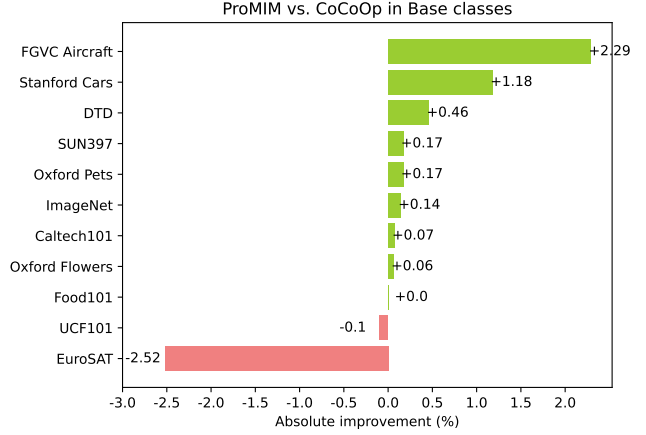
$\lambda$	0.0	1.0	<b>2.0</b>	4.0	6.0	8.0	10.0
H	76.15	76.58	<b>77.16</b>	76.87	76.37	76.53	76.57

## 5.5 Mask sampling strategy.

In Table 6b, we analyze mask sampling strategies. The *block-wise* strategy, introduced by [2], typically eliminates large contiguous sections. Our ProMIM, when using block-wise masking, performs adequately at a 50% ratio, but its effectiveness diminishes at 75%. This approach proves more difficult than random sampling due to an observed increase in training loss. Simple random sampling yields the best results for our ProMIM, as it supports a higher masking ratio, offering substantial speedup and maintaining high accuracy.

## 5.6 ProMIM enhances the generalization toward unseen classes

Figure 4 illustrates the absolute performance gains of ProMIM over CoCoOp, our primary comparison baseline. The addition of regularization constraints in ProMIM results in a slight reduction in accuracy on *Base* classes, as expected, due to the model’s reduced reliance on memorized class-specific features. However, we observe a consistent improvement in accuracy on 10 out of 11 datasets, especially with more than 10% improvement on the FGVC Aircraft dataset. These results underscore the ProMIM’s capability to debias the model from overfitting on *Base* classes, thereby enhancing its adaptability and generalization capability on unseen categories.

**(a) ProMIM consistently outperforms CoCoOp on unseen classes across all datasets.****(b) ProMIM reduces the overfitting effect, resulting in lower base performances.****Figure 4: Extensive evaluation of ProMIM versus CoCoOp in the context of base-to-new class generalization.**

## 6 Conclusion

Common CoOp-based prompt learning methods tend to overfit to classes encountered during fine-tuning, limiting their generalization to novel, unseen classes. To address this challenge, we introduce Masked Image Modeling-guided Conditional Prompt Learning (ProMIM), a flexible, plug-and-play framework that enhances prompt learning by integrating masked image modeling (MIM) into existing vision-language model (VLM) pipelines. ProMIM utilizes MIM's robust masking strategy to generate instance-conditioned prompts, effectively improving feature robustness and mitigating overfitting. This approach prevents data leakage from the visual to the textual branch, ensuring that the model establishes a stronger contextual framework for generating prompts. Evidence from various benchmarks and tasks confirms ProMIM's effectiveness and versatility, demonstrating its potential as a lightweight, practical solution for real-world vision-language applications.

## Acknowledgments

This work was partly supported by the Korea government (MSIT), IITP, Korea, under the ICT Creative Consilience program (IITP-2025-RS-2020-II201821, 30%), Development of Brain Disease (Stroke) Prediction Model based on Fundus Image Analysis (RS-2024-00459512, 30%), AI Innovation Hub (RS-2021-II212068, 20%), and AI Graduate School Program (Sungkyunkwan University, RS-2019-II190421, 20%).

## References

- [1] Jean-Baptiste Alayrac, Jeff Donahue, Pauline Luc, Antoine Miech, Iain Barr, Yana Hasson, Karel Lenc, Arthur Mensch, Katherine Millican, Malcolm Reynolds, et al. 2022. Flamingo: a visual language model for few-shot learning. *Advances in neural information processing systems* 35 (2022), 23716–23736.
- [2] Hangbo Bao, Li Dong, Songhao Piao, and Furu Wei. 2021. Beit: Bert pre-training of image transformers. *arXiv preprint arXiv:2106.08254* (2021).
- [3] Lukas Bossard, Matthieu Guillaumin, and Luc Van Gool. 2014. Food-101-mining discriminative components with random forests. In *Computer vision–ECCV 2014: 13th European conference, Zurich, Switzerland, September 6–12, 2014, proceedings, part VI 13*. Springer, 446–461.
- [4] Phuoc-Nguyen Bui, Duc-Tai Le, and Hyunseung Choo. 2024. Visual-textual matching attention for lesion segmentation in chest images. In *International Conference on Medical Image Computing and Computer-Assisted Intervention*. Springer, 702–711.
- [5] Ting Chen, Simon Kornblith, Mohammad Norouzi, and Geoffrey Hinton. 2020. A simple framework for contrastive learning of visual representations. In *International conference on machine learning*. PMLR, 1597–1607.
- [6] Jaemin Cho, Jie Lei, Hao Tan, and Mohit Bansal. 2021. Unifying vision-and-language tasks via text generation. In *International Conference on Machine Learning*. PMLR, 1931–1942.
- [7] Mircea Cimpoi, Subhransu Maji, Iasonas Kokkinos, Sammy Mohamed, and Andrea Vedaldi. 2014. Describing textures in the wild. In *Proceedings of the IEEE conference on computer vision and pattern recognition*. 3606–3613.
- [8] Jia Deng, Wei Dong, Richard Socher, Li-Jia Li, Kai Li, and Li Fei-Fei. 2009. Imagenet: A large-scale hierarchical image database. In *2009 IEEE conference on computer vision and pattern recognition*. Ieee, 248–255.
- [9] Alexey Dosovitskiy. 2020. An image is worth 16x16 words: Transformers for image recognition at scale. *arXiv preprint arXiv:2010.11929* (2020).
- [10] Li Fei-Fei, Rob Fergus, and Pietro Perona. 2004. Learning generative visual models from few training examples: An incremental bayesian approach tested on 101 object categories. In *2004 conference on computer vision and pattern recognition workshop*. IEEE, 178–178.
- [11] Peng Gao, Shijie Geng, Renrui Zhang, Teli Ma, Rongyao Fang, Yongfeng Zhang, Hongsheng Li, and Yu Qiao. 2024. Clip-adapter: Better vision-language models with feature adapters. *International Journal of Computer Vision* 132, 2 (2024), 581–595.
- [12] Kaiming He, Xinlei Chen, Saining Xie, Yanghao Li, Piotr Dollár, and Ross Girshick. 2022. Masked autoencoders are scalable vision learners. In *Proceedings of the IEEE/CVF conference on computer vision and pattern recognition*. 16000–16009.
- [13] Patrick Helber, Benjamin Bischke, Andreas Dengel, and Damian Borth. 2019. Eurosat: A novel dataset and deep learning benchmark for land use and land cover classification. *IEEE Journal of Selected Topics in Applied Earth Observations and Remote Sensing* 12, 7 (2019), 2217–2226.
- [14] Dan Hendrycks, Steven Basart, Norman Mu, Saurav Kadavath, Frank Wang, Evan Dorundo, Rahul Desai, Tyler Zhu, Samyak Parajuli, Mike Guo, et al. 2021. The many faces of robustness: A critical analysis of out-of-distribution generalization. In *Proceedings of the IEEE/CVF international conference on computer vision*. 8340–8349.
- [15] Dan Hendrycks, Kevin Zhao, Steven Basart, Jacob Steinhardt, and Dawn Song. 2021. Natural adversarial examples. In *Proceedings of the IEEE/CVF conference on computer vision and pattern recognition*. 15262–15271.
- [16] Chao Jia, Yinfel Yang, Ye Xia, Yi-Ting Chen, Zarana Parekh, Hieu Pham, Quoc Le, Yun-Hsuan Sung, Zhen Li, and Tom Duerig. 2021. Scaling up visual and vision-language representation learning with noisy text supervision. In *International conference on machine learning*. PMLR, 4904–4916.
- [17] Muhammad Uzair Khattak, Hanooona Rasheed, Muhammad Maaz, Salman Khan, and Fahad Shahbaz Khan. 2023. Maple: Multi-modal prompt learning. In *Proceedings of the IEEE/CVF Conference on Computer Vision and Pattern Recognition*. 19113–19122.
- [18] Muhammad Uzair Khattak, Syed Talal Wasim, Muzammal Naseer, Salman Khan, Ming-Hsuan Yang, and Fahad Shahbaz Khan. 2023. Self-regulating prompts: Foundational model adaptation without forgetting. In *Proceedings of the IEEE/CVF International Conference on Computer Vision*. 15190–15200.
- [19] Wonjae Kim, Bokyung Son, and Ilwoo Kim. 2021. Vilt: Vision-and-language transformer without convolution or region supervision. In *International conference on machine learning*. PMLR, 5583–5594.
- [20] Xiangwen Kong and Xiangyu Zhang. 2023. Understanding masked image modeling via learning occlusion invariant feature. In *Proceedings of the IEEE/CVF Conference on Computer Vision and Pattern Recognition*. 6241–6251.
- [21] Jonathan Krause, Michael Stark, Jia Deng, and Li Fei-Fei. 2013. 3d object representations for fine-grained categorization. In *Proceedings of the IEEE international conference on computer vision workshops*. 554–561.
- [22] Siting Li, Pang Wei Koh, and Simon Shaolei Du. 2024. On Erroneous Agreements of CLIP Image Embeddings. *arXiv:2411.05195 [cs.LG]* <https://arxiv.org/abs/2411.05195>
- [23] Pengfei Liu, Weizhe Yuan, Jinlan Fu, Zhengbao Jiang, Hiroaki Hayashi, and Graham Neubig. 2023. Pre-train, prompt, and predict: A systematic survey of prompting methods in natural language processing. *Comput. Surveys* 55, 9 (2023), 1–35.
- [24] Jiasen Lu, Dhruv Batra, Devi Parikh, and Stefan Lee. 2019. Vilbert: Pretraining task-agnostic visiolinguistic representations for vision-and-language tasks. *Advances in neural information processing systems* 32 (2019).
- [25] Chengcheng Ma, Yang Liu, Jiankang Deng, Lingxi Xie, Weiming Dong, and Changsheng Xu. 2023. Understanding and Mitigating Overfitting in Prompt Tuning for Vision-Language Models. *IEEE Transactions on Circuits and Systems for Video Technology* 33, 9 (2023), 4616–4629. doi:10.1109/TCST.2023.3245584
- [26] Subhransu Maji, Esa Rahtu, Juho Kannala, Matthew Blaschko, and Andrea Vedaldi. 2013. Fine-grained visual classification of aircraft. *arXiv preprint arXiv:1306.5151* (2013).
- [27] Maria-Elena Nilsback and Andrew Zisserman. 2008. Automated flower classification over a large number of classes. In *2008 Sixth Indian conference on computer vision, graphics & image processing*. IEEE, 722–729.
- [28] Omkar M Parkhi, Andrea Vedaldi, Andrew Zisserman, and CV Jawahar. 2012. Cats and dogs. In *2012 IEEE conference on computer vision and pattern recognition*. IEEE, 3498–3505.
- [29] Fabio Petroni, Tim Rocktäschel, Patrick Lewis, Anton Bakhtin, Yuxiang Wu, Alexander H Miller, and Sebastian Riedel. 2019. Language models as knowledge bases? *arXiv preprint arXiv:1909.01066* (2019).
- [30] Alex Radford, Jong Wook Kim, Chris Hallacy, Aditya Ramesh, Gabriel Goh, Sandhini Agarwal, Girish Sastry, Amanda Askell, Pamela Mishkin, Jack Clark, et al. 2021. Learning transferable visual models from natural language supervision. In *International conference on machine learning*. PMLR, 8748–8763.
- [31] Yongming Rao, Wenliang Zhao, Guangyi Chen, Yansong Tang, Zheng Zhu, Guan Huang, Jie Zhou, and Jiwen Lu. 2022. Denseclip: Language-guided dense prediction with context-aware prompting. In *Proceedings of the IEEE/CVF conference on computer vision and pattern recognition*. 18082–18091.
- [32] Benjamin Recht, Rebecca Roelofs, Ludwig Schmidt, and Vaishaal Shankar. 2019. Do imagenet classifiers generalize to imagenet? In *International conference on machine learning*. PMLR, 5389–5400.
- [33] Sheng Shen, Shijia Yang, Tianjun Zhang, Bohan Zhai, Joseph E Gonzalez, Kurt Keutzer, and Trevor Darrell. 2024. Multitask vision-language prompt tuning. In *Proceedings of the IEEE/CVF Winter Conference on Applications of Computer Vision*. 5656–5667.
- [34] Lingxue Song, Dihong Gong, Zhifeng Li, Changsong Liu, and Wei Liu. 2019. Occlusion robust face recognition based on mask learning with pairwise differential siamese network. In *Proceedings of the IEEE/CVF international conference on computer vision*. 773–782.

[35] Khurram Soomro, Amir Roshan Zamir, and Mubarak Shah. 2012. UCF101: A dataset of 101 human actions classes from videos in the wild. *arXiv preprint arXiv:1212.0402* (2012).

[36] Maria Tsimpoukelli, Jacob L Menick, Serkan Cabi, SM Eslami, Oriol Vinyals, and Felix Hill. 2021. Multimodal few-shot learning with frozen language models. *Advances in Neural Information Processing Systems* 34 (2021), 200–212.

[37] Haohan Wang, Songwei Ge, Zachary Lipton, and Eric P Xing. 2019. Learning robust global representations by penalizing local predictive power. *Advances in Neural Information Processing Systems* 32 (2019).

[38] Zirui Wang, Jiahui Yu, Adams Wei Yu, Zihang Dai, Yulia Tsvetkov, and Yuan Cao. 2021. Simvlm: Simple visual language model pretraining with weak supervision. *arXiv preprint arXiv:2108.10904* (2021).

[39] Ge Wu, Xin Zhang, Zheng Li, Zhaowei Chen, Jiajun Liang, Jian Yang, and Xiang Li. 2024. Cascade prompt learning for vision-language model adaptation. In *European Conference on Computer Vision*. Springer, 304–321.

[40] Jianxiong Xiao, James Hays, Krista A Ehinger, Aude Oliva, and Antonio Torralba. 2010. Sun database: Large-scale scene recognition from abbey to zoo. In *2010 IEEE computer society conference on computer vision and pattern recognition*. IEEE, 3485–3492.

[41] Hantao Yao, Rui Zhang, and Changsheng Xu. 2023. Visual-language prompt tuning with knowledge-guided context optimization. In *Proceedings of the IEEE/CVF conference on computer vision and pattern recognition*. 6757–6767.

[42] Hantao Yao, Rui Zhang, and Changsheng Xu. 2024. TCP: Textual-based Class-aware Prompt tuning for Visual-Language Model. In *Proceedings of the IEEE/CVF Conference on Computer Vision and Pattern Recognition*. 23438–23448.

[43] Ji Zhang, Shihan Wu, Lianli Gao, Heng Tao Shen, and Jingkuan Song. 2024. Dept: Decoupled prompt tuning. In *Proceedings of the IEEE/CVF Conference on Computer Vision and Pattern Recognition*. 12924–12933.

[44] Kaiyang Zhou, Jingkang Yang, Chen Change Loy, and Ziwei Liu. 2022. Conditional prompt learning for vision-language models. In *Proceedings of the IEEE/CVF conference on computer vision and pattern recognition*. 16816–16825.

[45] Kaiyang Zhou, Jingkang Yang, Chen Change Loy, and Ziwei Liu. 2022. Learning to prompt for vision-language models. *International Journal of Computer Vision* 130, 9 (2022), 2337–2348.

[46] Beier Zhu, Yulei Niu, Yucheng Han, Yue Wu, and Hanwang Zhang. 2023. Prompt-aligned gradient for prompt tuning. In *Proceedings of the IEEE/CVF International Conference on Computer Vision*. 15659–15669.